JOURNAL OF CATALYSIS 147, 567–577 (1994)

Carbon Monoxide Oxidation over Three Different Oxidation States of Copper: Metallic Copper, Copper (I) Oxide, and Copper (II) Oxide—A Surface Science and Kinetic Study

G. G. Jernigan* and G. A. Somorjai†

*Department of Chemistry and †Material Science Division, Lawrence Berkeley Laboratory, University of California, Berkeley, California 94720

Received November 9, 1993; revised January 25, 1994

Reaction rates and activation energies were measured for carbon monoxide oxidation over thin films of metallic copper, copper (I) oxide, and copper (II) oxide grown on graphite. The reactions were carried out in the temperature range 200–350°C at total pressures of 100 Torr. Auger Electron Spectroscopy (AES) and X-ray Photoelectron Spectroscopy (XPS) were used to characterize the growth and oxidation states of the copper films before and after catalytic reactions. The stability of a given oxidation state of copper under reaction conditions was found to be a function of the oxidizing power of the CO/O_2 partial pressure ratio: metallic copper, Cu_2O, and CuO were stable at 97/3, 90/10, and 66/33 ratios, respectively. The rate of reaction at 300°C decreased with increasing copper oxidation state ($Cu > Cu_2O > CuO$) and the activation energy increased with increasing copper oxidation state ($Cu\ 9 < Cu_2O\ 14 < CuO\ 17$ kcal/mol). The kinetic parameters for CO oxidation over platinum foil was tested at a 66/33 CO/O_2 ratio for comparison. The reaction rate over platinum was approximately equal to that over metallic copper at 300°C and had a larger activation energy (20 kcal/mol) than CuO. The possible mechanisms for CO oxidation over the different oxidation states of copper are discussed. © 1994 Academic Press, Inc.

INTRODUCTION

Oxidation of carbon monoxide over copper catalysts is significant in understanding methanol synthesis, the water–gas shift reaction, and automotive exhaust controls, to mention a few major applications. Studies have shown that methanol synthesis is likely to occur by the hydrogenation of carbon dioxide and that carbon monoxide is needed to scavenge oxygen left on the surface (1, 2). In the water gas shift reaction, carbon monoxide removes surface hydroxyls or oxygen produced by the dissociation of water (3, 4). Copper has been explored as a possible substitute for palladium and platinum for the reduction of nitrogen oxides by carbon monoxide in automotive catalytic converters (5, 6). The reaction is believed to occur through the decomposition of NO_x to form nitrogen gas and adsorbed oxygen on the surface; the oxygen then reacts with carbon monoxide. Even though the importance of the oxidation of carbon monoxide over copper has been recognized, the reaction remains poorly understood because of changes in the copper oxidation state as the reaction conditions are altered. It is usually assumed that copper is active in a particular oxidation state, or in the case of a redox reaction, that it cycles between two oxidation states. To date, there has been no attempt to investigate how the rate of a reaction varies as a function of copper oxidation state.

We report here the first high pressure study of carbon monoxide oxidation on model low surface area copper and copper oxide surfaces:

$$CO + \tfrac{1}{2}O_2 \xrightarrow[Cu_2O]{Cu} CO_2.$$
$$\xrightarrow[CuO]{}$$

We studied the catalytic oxidation of carbon monoxide over copper in such a way that by adjusting the CO/O_2 partial pressure ratio in the reactant mixture and the temperature we could fix the oxidizing power. Within certain ranges of CO/O_2 we could stabilize the copper catalyst in its zero, +1, or +2 oxidation state. The catalyst was a thin film of copper deposited onto a graphite support under ultrahigh vacuum (UHV). In this way the copper oxidation state throughout the film would be uniform, as the sample could rapidly equilibrate to the oxidation state imposed by the CO/O_2 ratio and could be measured.

Studies of carbon monoxide oxidation on copper by others have been performed under high vacuum using single crystals (6–10) and also supported copper catalysts (11–17). The single crystal studies react carbon monoxide at pressures less than or equal to 1×10^{-4} Torr with saturation coverages of oxygen predosed on the copper surface. In these cases the reaction conditions are very

0021-9517/94 $6.00

reducing (CO/O_2 ratio greater than 100) in order to maintain a metallic surface. There is little information from these studies on how the reaction and surface change when higher pressures and more oxidizing conditions are used. Additionally, the reaction on the single crystal typically turns over only once. Therefore, the reaction is not catalytic. Carbon monoxide oxidation performed on supported copper catalysts was studied under total pressures between 10 and 760 Torr with an oxidizing gas mixture (CO/O_2 ratios less than the stoichiometric value of 2). The catalysts were formed first by calcining a copper salt to copper (II) oxide (CuO). The catalyst is either used in this state or pretreated. The pretreatment result in a reduction of the catalyst to metallic copper, copper (I) oxide (Cu_2O), or a mixed oxide typically measured by bulk X-ray diffraction prior to the reaction. These studies do not determine the surface oxidation state of the copper.

This paper bridges the gap between the low pressure single crystal studies and the studies of the supported catalysts that were carried out at high pressures. Copper and its oxides were investigated in this study using surface science techniques and a high pressure reactor under reaction conditions where the CO/O_2 ratios overlap the conditions utilized in both single crystal and supported catalyst studies. To do this we constructed in our laboratory a special high pressure reactor and transfer system which was capable of operating under oxidizing conditions and connected it to a UHV chamber. We carried out CO oxidation at 100 Torr total pressure and CO/O_2 ratios between 2 and 100 over the temperature range 200–350°C. X-ray Photoelectron Spectroscopy (XPS) and Auger Electron Spectroscopy (AES) were used to characterize metallic copper, copper (I) oxide, and copper (II) oxide that were deposited onto a graphite support. Reactions were also performed using platinum foil to provide a reference for the activity of the copper surfaces in their different oxidation states.

We find that the reaction rate of CO oxidation is fastest on metallic copper, and at 300°C the rate decreases with increasing copper oxidation state: Cu (0) > Cu (+1) > Cu (+2). The apparent activation energies for the reaction increases in a similar order: 9 kcal/mol Cu (0) < 14 kcal/mol Cu (+1) < 17 kcal/mol Cu (+2). The reaction rate on platinum at 300°C was approximately equal to the rate on metallic copper but was greater then the rates for the oxides of copper. The activation energy, 20 kcal/mol, for the reaction on platinum was greater than for the reactions on the three copper samples. The different activation energies obtained for the reaction on copper in different oxidation states indicates a changing mechanism that will be discussed. We hope that these studies will aid the development of a better understanding of the role played by copper in catalytic reactions in its various oxidation states.

EXPERIMENTAL

(A) *Apparatus*

Experiments were performed in a stainless steel MDC manufactured ultrahigh vacuum (UHV) chamber. The chamber was equipped with a Perkin–Elmer 15-25G double pass cylindrical mirror analyzer with an integral electron gun, a Perkin–Elmer 04-548 dual anode (Al/Mg) X-ray source, a Varian 981-2043 sputter ion gun, a UTI 100C quadrupole mass spectrometer, and an external atmospheric pressure reaction cell. The sample was mounted on a transfer piece which consisted of four pins in an alumina holder. Two pins were stainless steel, the sample was attached across them for resistive heating. The other two were an alumel and chromel pair for making a type K thermocouple. The transfer piece mated into manipulators in the UHV chamber and in the reaction cell. The sample was prepared and analyzed in UHV, then shuttled to the reaction cell using a transfer rod. The chamber depicted in Fig. 1 was pumped by an oil diffusion pump and a titanium sublimation pump and had a base pressure of 2×10^{-10} Torr, uncorrected. The high pressure cell withstood pressures up to 2 atmospheres and was pumped by a sorption pump and a mechanical pump. A gate valve separated the UHV chamber and reaction cell, and when opened, the base pressure measured in the UHV chamber rose to 1×10^{-8} Torr.

(B) *Sample Preparation*

The sample was a $1 \times 1 \times 0.005$ cm graphite coated stainless steel foil onto which copper was deposited, or a $1 \times 1 \times 0.005$ cm platinum foil. The platinum foil was used for comparison purposes. The graphite coated stainless steel foil was prepared by cleaning a 304 stainless steel foil with methanol then spraying it with Aerodag (a registered trademark of Acheson) and allowed to dry. Aerodag is a dry film lubricant of micron-sized graphite particles suspended in isopropyl alcohol, per the label. The thermal stability of Aerodag was tested by heating a sample in pure oxygen (100 Torr). No CO_2 was produced at temperatures less than 450°C and AES showed no delamination of the graphite coating. Prior to copper deposition, the foil was annealed at 600°C in UHV to remove any remaining alcohol and surface oxygen species.

Copper was deposited by evaporation from an alumina crucible. The crucible was heated to 1500°C by passing current through a tungsten wire wrapped around the outside. The crucible was heated for 20 min prior to deposition to assure a steady flux of copper atoms. A deposition

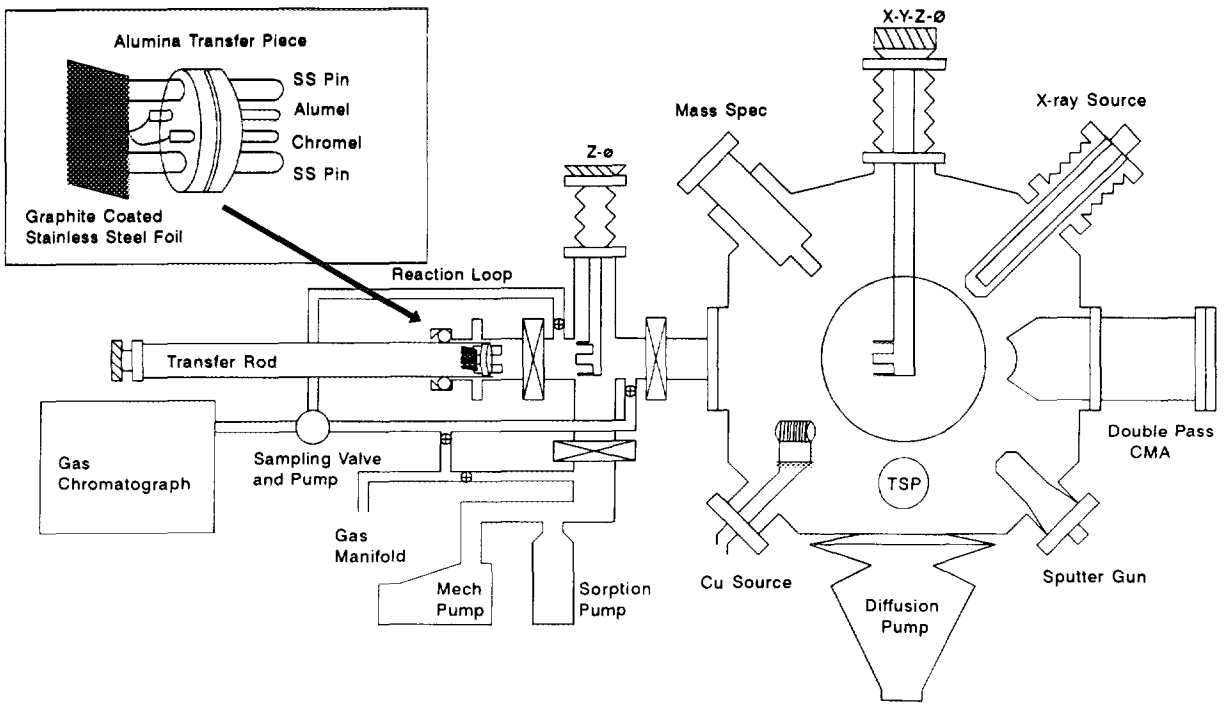

FIG. 1. Schematic diagram of ultra high vacuum chamber designed for this experiment.

rate of approximately 0.5 monolayers per minute was measured by an AES uptake curve of Cu deposited onto a pure Fe foil. The deposition of 10 monolayers of metallic copper was the first stage in the preparation of all of the copper catalysts used in these experiments. The freshly deposited copper was used as is for the metallic copper measurements. Copper (II) oxide was produced by oxidizing the metallic copper in the reaction cell in 100 Torr of oxygen at 300°C for 20 min. Copper (I) oxide was obtained by annealing copper (II) oxide in UHV at 400°C for 10 min. The platinum foil was cleaned by repeated cycles of sputtering at 1500 V in 1×10^{-5} Torr of argon at 600°C, heating in oxygen at 600°C, and briefly annealing at 700°C.

(C) Experimental Procedure

Auger and X-ray photoelectron spectra were taken before and after each catalytic run. The spectra were acquired by a personal computer. AES were taken using a 2 keV primary beam energy with a 1 mA emission current and approximately a 30 μA beam current. The analyzer control had a 4 V peak to peak modulation and was scanned at 100 ms per eV from 1 to 1000 eV. XPS were taken at 400 W with both the magnesium anode ($h\nu$ = 1253.6 eV) and the aluminum anode ($h\nu$ = 1486.6 eV). The Cu $2P$ and LVV regions, along with the O $1S$ region, were scanned using a CMA pass energy of 25 eV. Each region was signal averaged for 20 scans at 200 ms per eV. The XPS binding energies were referenced to the graphite C $1S$ peak at 284.2 eV and the system was occasionally checked using the Fe $2P_{3/2}$ peak at 706.8 eV of a sputtered cleaned pure iron foil.

Reactions were run between 200 and 350°C in a batch reactor with a volume of 0.68 liter. The sample was resistively heated during the reaction using a Eurotherm temperature controller which maintained the sample temperature to within 1°C over the course of the reaction. CO and O_2 were premixed in a separate vessel in partial pressure ratios of 66/33, 90/10, and 97/3, CO to O_2, respectively, before admittance to the reactor. CO (Airco grade 2.3) was distilled with 5 Å molecular sieve trap in a liquid nitrogen bath to remove metal carbonyls prior to use, and O_2 (Airco grade 2.6) was used without purification. For each reaction a total of 100 Torr of mixed gas was used. The gases were recirculated in the reactor at 100 cm^3/min. The sample was brought to the reaction temperature in the presence of the gases in approximately 4 min. The production of CO_2 and the decrease of CO and O_2 were monitored by gas chromatography using a Supelco Carboxen 1000 column run isothermally at 125°C with a helium carrier flow of 30 ml/min and measured by a thermal conductivity detector. The sensitivity of the thermal conductivity detector was calibrated using known partial pressures of the individual gases. A 1-ml aliquot gas sample was removed by an automatic sampling valve every 11 min. and injected into the gas chromatograph.

After the reaction, the cell was pumped to less than 50 mTorr; then it was transferred into UHV. A 10 min. delay was necessary to allow the base pressure to return to less than 1×10^{-9} Torr before post reaction analysis was performed.

RESULTS

(A) *Catalyst Characterization by AES and XPS*

The AES of graphite coated stainless steel is depicted in Fig. 2. The sample was introduced to UHV and annealed at 600°C. The absence of an oxygen peak is due to removal of carboxyl and hydroxyl groups from the graphite surface (18) by annealing. The Auger peaks for Fe, Cr, and O of the stainless steel substrate are not seen. A post blank reaction of a graphite coated stainless steel foil exposed to a 66/33 CO/O_2 ratio at 300°C for 2 hr is also shown in Fig. 2. It contains a small oxygen signal which disappears upon annealing at temperatures greater than 300°C. One reason for choosing graphite as a substrate was that it could be cleaned of oxygen and does not readily oxidize. Hence, any oxygen signal appearing in the AES or XPS could be associated with oxygen bound to copper. Graphite is also highly conductive, which allowed the electron spectroscopies to be performed without sample charging difficulties.

A 20-min. copper deposition onto the graphite coated substrate resulted in an attenuation of the carbon peak, as seen in Fig. 2. This corresponds to approximately 10 monolayers. An AES uptake curve of Cu 918 eV peak intensity versus deposition time did not show any distinct breaks but followed a smooth curve, indicative of a Volmer–Weber growth mode (island formation). With the oxidation of metallic copper to copper (I) oxide, the carbon 272 eV peak intensity decreased further while the copper 918 eV peak remained unchanged. We interpreted this to be due to the spreading of the copper (I) oxide islands on the graphite. Upon further oxidation to copper (II) oxide, there was an additional decrease in the carbon peak without a change in the copper peak, indicative of further spreading of the oxide islands on the graphite. These observations are consistent with a progressive decrease in the surface tension of the islands as the copper is oxidized. As the surface tension decreases, the islands wet the graphite surface. This model is valid if the interfacial energy between the islands and graphite is small, and that would be expected based on the chemical inertness of graphite.

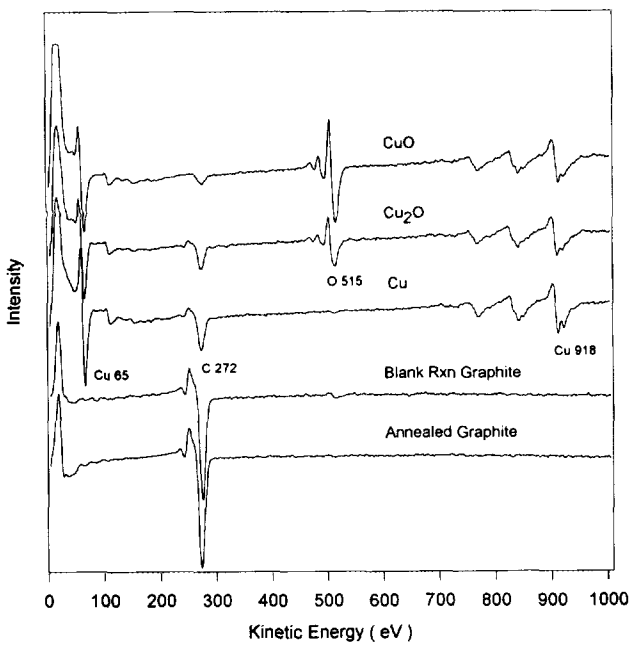

FIG. 2. AES of an annealed graphite substrate, a graphite substrate after a blank reaction run under a 66/33 CO/O_2 ratio at 300°C for 2 hr, and catalyst films of metallic copper, copper (I) oxide, and copper (II) oxide grown on graphite.

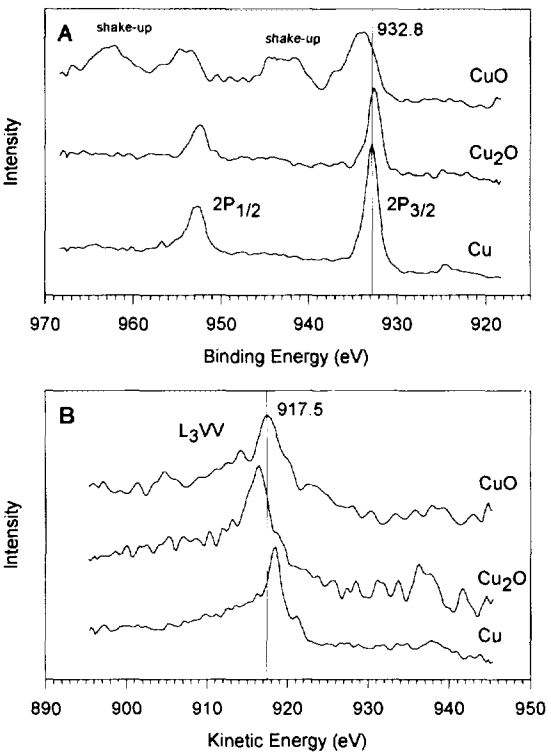

FIG. 3. XPS of (A) Cu $2P$ and (B) Cu LVV regions for the metallic copper, copper (I) oxide, and copper (II) oxide references used in these experiments.

Figure 3 shows the copper $2P$ and LVV XPS peaks for metallic copper, copper (I) oxide, and copper (II) oxide prepared for these experiments and used as reference. Spectroscopically, the different oxidation states of copper can be distinguished by their Auger parameter (the sum of the $2P_{3/2}$ binding energy and the LVV kinetic energy)

as well as by the presence of shake-up peaks for copper (II) oxide (19–23). Table 1 lists the Auger parameter data. AES relative peak intensities of the oxygen 515 eV peak to the copper 918 eV peak can also be used for quantitative analysis of stoichiometry. Auger copper to oxygen ratios are listed in Table 1 for copper (I) oxide and copper (II) oxide.

Using the reference data, one can readily study the oxidation of metallic copper. The results of exposing a metallic copper surface to a 66/33 Torr CO/O_2 gas mixture at 275°C are shown in Fig. 4, curves (a)–(g). Curve (a) is the initially deposited metallic copper and each subsequent curve, (b) through (g), is an 11-min exposure totaling 66 min. for the experiment. For the first exposure, curve (a) to (b), there was a significant shift to lower kinetic energies for the Cu LVV transition seen in Fig. 4B. The Cu $2P_{3/2}$ peak shifts to slightly lower binding energies for the first exposure, curve (a) to (b) in Fig. 4A. Exposures (b) through (g) show a gradual shift back to higher kinetic energies for the Cu LVV peak. The Cu $2P_{3/2}$ peak shifts to higher binding energies for exposures (b) through (g), and the shake-up peak increases in intensity with each exposure. The changes in the spectra are consistent with metallic copper being oxidized to copper (I) oxide for exposures (a) to (b) and copper (I) oxide being oxidized to copper (II) oxide for exposures (b) through (g). This finding agrees well with other studies of the oxidation of copper (22, 23). All exposures produced CO_2. The amount of CO_2 produced decreased with increasing exposure, showing that metallic copper, copper (I) oxide, the partial oxides between copper (I) and copper (II), and copper (II) oxide were all active for CO oxidation.

(*B*) *Catalytic Reaction Studies*

Catalytic reactions were performed with different CO to O_2 partial pressure ratios for metallic copper, copper (I) oxide, and copper (II) oxide using 97/3, 90/10, and 66/33, respectively, because the surface oxidation state can change as a function of the gas composition, temperature, and exposure time. These ratios were chosen because in each case the 300°C post-reaction XPS indicated that the copper oxidation state had not changed from the oxidation state prior to the reaction. By performing CO oxidation under conditions where the oxidation state of the catalyst does not change, we were able to obtain activation energies for the three different oxidation states of copper. Platinum was tested under a CO/O_2 ratio of 66/33. The results are reported as the percentage of CO in the reactor that was converted to CO_2 versus time, defined as

$$\%CO = \left(\frac{P_{CO_2}}{P_{CO} + P_{CO_2}}\right),$$

where P_{CO} and P_{CO_2} are the partial pressures of CO and CO_2, respectively. Rates obtained from the initial slopes of percentage of CO converted versus time were used to calculate the activation energy for CO oxidation.

TABLE 1

Reference Values for Metallic Copper, Cuprous Oxide, and Cupric Oxide

	Auger Ratio O/Cu[a]	Cu $2P_{3/2}$ Binding Energy	Cu LVV Kinetic Energy	Auger Parameter
Metallic copper	—	932.8	918.5	1851.3
Cuprous oxide	1.1	932.6	916.5	1849.1
Cupric oxide	2.3	933.8 (SU)	917.6	1851.4

[a] 3keV beam energy (SU) Shake up at 942.5 eV.

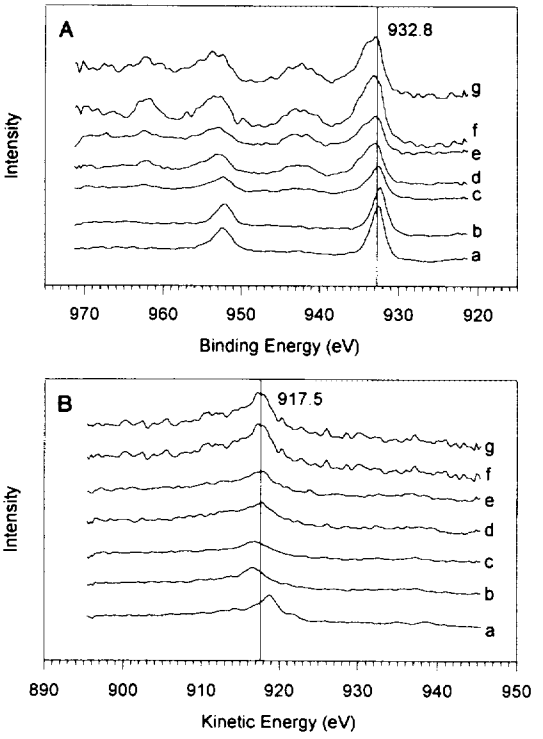

FIG. 4. XPS of (A) Cu 2*P* and (B) Cu LVV regions for a metallic copper catalyst exposed to a 66/33 CO/O_2 gas mixture at 275°C for a cumulative time of (a) 0, (b) 11, (c) 22, (d) 33, (e) 44, (f) 55, and (g) 66 min.

(*1*) *Metallic copper catalyst.* Representative kinetic data for CO oxidation on a metallic copper catalyst are shown in Fig. 5A. A CO/O_2 ratio of 97/3 was used and could result in a maximum CO conversion of 6.2%, where O_2 is the limiting reagent. There was a rapid rise in conversion for curves (a) 350, (b) 300, and (c) 275°C, resulting in the complete use of oxygen. At 200°C, curve (e), the initial rate is not rapid but gradually rises. The 250°C data, curve (d), show a slow initial rate but at 89 min. there is

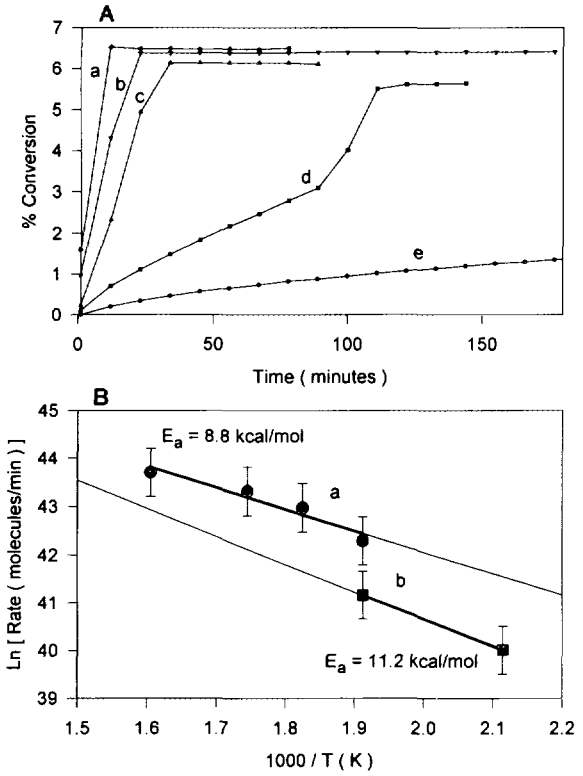

FIG. 5. CO oxidation results for a metallic copper catalyst run under a 97/3 CO/O_2 gas mixture. The maximum CO conversion is 6.2%. (A) Percent of CO converted to CO_2 versus time for (a) 350, (b) 300, (c) 275, (d) 250, and (e) 200°C. (B) Arrhenius plots for (a) an oxygen free metallic copper catalyst using the initial CO oxidation rates of the catalytic runs at 350, 300, and 275°C, and the rapid rise in the 250°C catalytic run, and (b) an oxidized metallic copper catalyst using the initial CO oxidation rates for the 200 and 250°C catalytic runs.

a rapid rise in the percent conversion. A comparison of the XPS and Auger spectra before and after the change in activity for the 250°C reaction shows that the rapid rise is due to the copper becoming metallic. Hence, even under these very reducing conditions, the catalyst is slightly oxidized upon exposure to the reactant gas mixture. The reduction of the surface is very slow at temperatures below 250°C. Using the reaction rate where the catalyst is known to be metallic, curves (a), (b), (c), and (d) after the break, gave an activation energy of 8.8 ± 1.0 kcal/mol for CO oxidation on the metallic copper catalyst in Fig. 5B. This is in good agreement with UHV studies of CO oxidation on copper single crystals (8–10). Using the reaction rate where the surface is oxidized, curve (e) and curve (d) before the break gave a higher activation energy of 11.2 ± 1.0 kcal/mol. The error in the activation energies for the metallic copper catalysts are large because of the few points available in calculating the slope for the rapid rise of the high temperature reactions and in the very low conversion for the reactions at the lower temperatures.

(2) Copper (I) oxide catalyst. Representative kinetic data for CO oxidation on a copper (I) oxide catalyst are shown in Fig. 6A. A ratio of 90/10 was used and could result in a maximum CO conversion of 22.2% based on complete use of gas phase oxygen. The kinetic curves, (a) 350, (b) 300, (c) 275, (d) 250, and (e) 200°C, are smoothly varying with time. This indicates that there is no change in the catalyst oxidation state such as was seen in the metallic copper catalyst data. The 350°C run does approach complete use of the gas phase oxygen. XPS showed that for an extended run at 350°C the catalyst surface does not reduce until all of the gas phase oxygen had been consumed. Using the initial reaction rates an apparent activation energy of 13.9 ± 0.5 kcal/mol for CO oxidation on copper (I) oxide was calculated. The Arrhenius plot for copper (I) oxide is shown in Fig. 6B.

(3) Copper (II) oxide catalyst. Representative data for CO oxidation on a copper (II) oxide catalyst are shown in Fig. 7A. A CO/O_2 ratio of 66/33 was used and could result in a CO conversion of 100% based on complete use of gas phase oxygen. The kinetic curves, (a) 350, (b) 300, (c) 275, (d) 250, and (e) 200°C, have fast initial rates. For all the curves, at 22 min. the rates begin to decrease.

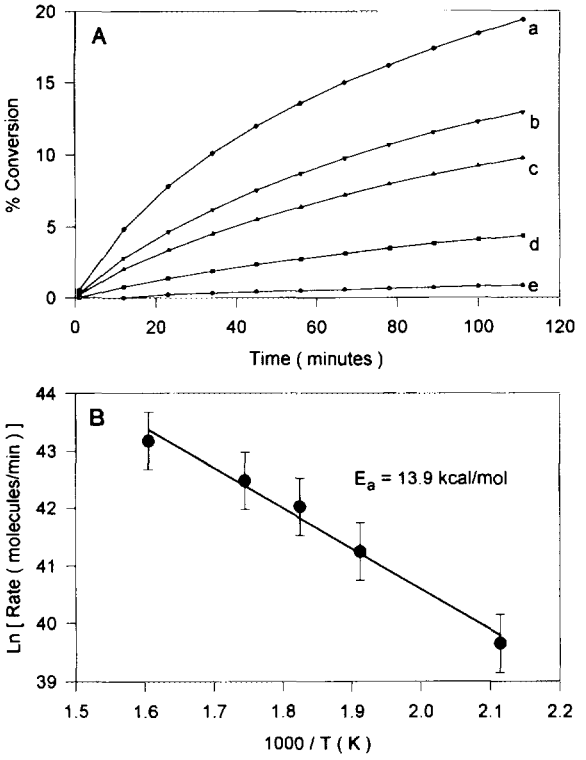

FIG. 6. CO oxidation results for a copper (I) oxide catalyst run under a 90/10 CO/O_2 gas mixture. The maximum CO conversion is 22.2%. (A) Percent of CO converted to CO_2 versus time for (a) 350, (b) 300, (c) 275, (d) 250, and (e) 200°C. (B) Arrhenius plot for a copper (I) oxide catalyst using the initial CO oxidation rates of the catalytic runs.

Extended catalyst runs beyond 2 hr resulted in complete deactivation of the catalyst. The catalyst does not completely use all of the gas phase oxygen present. This deactivation is believed to be due to CO_2 adsorption onto the surface (14). Post reaction XPS did not show the presence of a carbonate peak. After deactivation, the reaction cell was evacuated and admittance of fresh gases returned the catalyst to its initial activity. Hence, we believe that CO_2 does not modify the catalyst surface, but does block adsorption sites. Using the initial reaction rates an apparent activation energy of 16.7 ± 0.5 kcal/mol for CO oxidation on the copper (II) oxide was determined. The Arrhenius plot is shown in Fig. 7B. This is in good agreement with supported catalyst measurements (12, 13).

(4) Platinum catalyst. Representative kinetic data for CO oxidation on a platinum foil are shown in Fig. 8A. A CO/O_2 ratio of 66/33 was used resulting in a maximum CO conversion of 100%. The reaction at 350°C, curve (a), has a very large initial rate and slowly decreases as the reaction approaches 100% conversion. At lower temperatures, the curves, (b) 300, (c) 275, (d) 250, and (e) 200°C, are nearly linear with time with the initial rate being slightly greater. Extended runs at 300°C resulted in complete use of CO and O_2. Post reaction AES for all temperatures did not show any surface oxygen present. Using the initial reaction rates an apparent activation energy of 19.9 ± 0.5 kcal/mol for CO oxidation was determined from an Arrenhius plot, shown in Fig. 8B. The apparent activation energy is in close approximation to the values reported for similar temperatures and gas pressures for CO oxidation in a flow reactor (24).

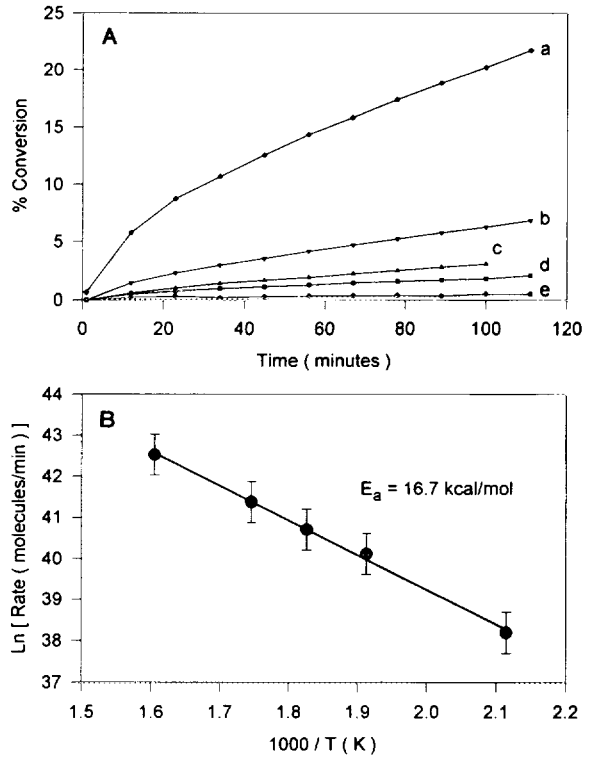

FIG. 7. CO oxidation results for a copper (II) oxide catalyst run under a 66/33 CO/O_2 gas mixture. The maximum CO conversion is 100%. (A) Percent of CO converted to CO_2 versus time for (a) 350, (b) 300, (c) 275, (d) 250, and (e) 200°C. (B) Arrhenius plot for a copper (II) oxide catalyst using the initial CO oxidation rates of the catalytic runs.

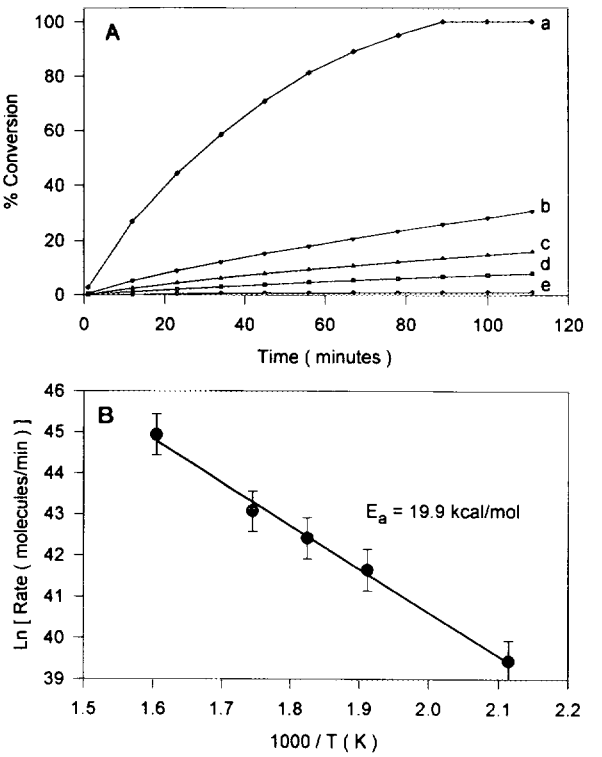

FIG. 8. CO oxidation results for a platinum catalyst run under a 66/33 CO/O_2 gas mixture. The maximum CO conversion is 100%. (A) Percent of CO converted to CO_2 versus time for (a) 350, (b) 300, (c) 275, (d) 250, and (e) 200°C. (B) Arrhenius plot for a platinum catalyst using the initial CO oxidation rates of the catalytic runs.

DISCUSSION

(A) Surface Reduction and Oxidation

This work has been motivated by the lack of knowledge concerning how a catalyst's surface oxidation state affects its catalytic ability and whether the changes in the surface oxidation are part of the catalytic mechanism. This is especially important in selective oxidation and combustion reactions over mixed metal oxide catalysts. For these reactions, it is commonly proposed that the reaction mechanism does occur through a redox cycle. The initial step in the reaction is the reduction of the surface by a gas phase reactant. The oxidized reactant can then undergo

rearrangements prior to leaving the surface. The final step in the reaction is the reoxidation of the catalyst by gas phase oxygen. This mechanism has yet to be experimentally verified but there are some reports which strongly suggest (25) that it is valid. The obstacle to experimentally determining this reaction mechanism has been the inability to monitor the surface oxidation state. This is difficult because there is a rapid reoxidation of the surface by the gas phase and by diffusion of bulk oxygen to the catalyst surface.

We circumvent these difficulties by using a thin (10 monolayers) copper catalyst. In this way the whole catalyst can be viewed as a surface without different bulk properties. The use of a bulk sample would have resulted in a reservoir for oxygen or metallic copper. A thick film would not be appropriate because the electron spectroscopies have a limited penetration depth into the surface. This has importance in studying metallic copper, where oxygen can go into the near surface region (26). As was demonstrated in the kinetic results for CO oxidation over metallic copper at 250°C, the presence of subsurface oxygen can affect the reaction rate.

The success of using a thin copper catalyst is also demonstrated in the time exposure of a metallic copper catalyst to a 66/33 CO/O_2 ratio at 275°C seen in Fig. 4. There is competition between the oxidation of the catalyst surface and the oxidation of CO. We are seeing the kinetics of surface oxidation on a time scale which is much greater than the kinetics of CO oxidation. Knowing that there can be a solid state reaction, and working to avoid it, allows us to better understand how the reaction is occurring over the different copper catalysts.

(b) Mechanistic Considerations

Working with gas mixtures of CO and O_2, where the catalyst composition does not change on the time scale of the reaction, we are able to compare the activity and activation energies for the different oxidation states of copper. Different rate-determining steps for each of the oxidation states of copper could be inferred from having obtained different activation energies. The rate determining step could be (1) adsorption of species onto different sites for each surface, (2) reactions between adsorbed species, (3) reactions between adsorbed species and the catalyst surface, (4) reactions between adsorbed species and the gas phase, and (5) reaction between the catalyst surface and the gas phase. Let us consider which of these steps might control the rate for a given copper oxidation state.

(1) Reactions over metallic copper. We believe that the mechanism of CO oxidation over the metallic copper catalyst is of the Langmuir-Hinshelwood type and that the presence of oxygen affects the adsorption of CO. Our kinetic results showed that the reaction had different rates when there was surface oxygen present. The rate of CO oxidation was slower on an oxidized surface. Surface oxygen was found during reactions run at temperatures less than 275°C. With time, the oxidized surfaces were gradually reduced. Upon the return to a metallic oxidation state, the rate of reaction increased over the metallic copper surface. For reactions run at temperatures greater than 275°C, the surface did not oxidize and had a faster rate for CO oxidation than the oxidized surface. This changing rate had been seen by O. P. van Pruissen (10), who attributed it to two different sites for oxygen, surface and subsurface. The reaction is limited by the adsorption of CO, which was postulated to be inhibited by surface oxygen. At the start of the reaction, there is a low surface coverage of CO. The CO reacts with the surface oxygen, which is replenished by subsurface oxygen. When the bulk is depleted of subsurface oxygen, the concentration of CO on the surface can increase. The reaction rate changes because adsorbed CO does not inhibit the adsorption of O_2. Hence, gas phase O_2 can react rapidly upon adsorption with the CO present. We agree with that interpretation of the change in the reaction rate. XPS results did show that oxygen was present when the reaction rate was slow and absent when the reaction rate was fast. This fits well with other UHV studies in the literature which postulate that the reaction mechanism can be described with the Langmuir–Hinshelwood model (9). For metallic copper the reaction rate is different over an oxygen saturated surface and a carbon monoxide saturated surface.

(2) Reactions over copper (I) oxide. Studies of the mechanism of CO oxidation over copper (I) oxide are complicated by many subtleties. Copper (I) oxide is only stable under a small range of CO/O_2 ratios. A smaller CO/O_2 ratio would result in the oxidation of the surface and a higher ratio would result in a reduction of the surface. During the course of a reaction, the CO/O_2 ratio will increase as the limiting reagent, oxygen, is depleted. The surface will most likely be reduced at a point in the reaction. A second difficulty arises from the possibility that the reaction might undergo a redox cycle involving the surface oxidation state. The mechanism could cycle between Cu_2O and CuO, where the first step in the reaction is the oxidation of the surface, or the mechanism could cycle between Cu_2O and metallic copper, where the first step in the reaction would be the reduction of the surface. The last concern is if the reaction does not involve a change in the oxidation state of the surface how does the reaction proceed? There have been very few surface science or catalysis studies on copper (I) oxide in the literature.

From the kinetic curves obtained for the reaction of a 90/10 CO/O_2 ratio over copper (I) oxide, some insight can

be gained. First, the curves are smoothly varying with time. This most likely indicates that there is not a change in the reaction mechanism as was seen over a metallic copper catalyst. Second, it was discovered that the surface did not reduce until all gas phase oxygen had been reacted. This is also in contrast to what occurs over metallic copper. These two facts discount a redox cycle between metallic copper and copper (I) oxide. If the redox cycle was occurring, as oxygen was being removed from the gas phase, fewer sites would be reoxidized to copper (I) oxide. Therefore, as the reaction proceeded, the surface would gradually become reduced to metallic copper. This does not occur, because we do not see any reduction in the surface during the reaction. Last, there is no deactivation in the catalyst. The formation of CO_2 does not inhibit the reaction.

We propose that the mechanism of CO oxidation over copper (I) oxide is of the Langmuir–Hinshelwood type and is related to the metallic copper catalyst case where subsurface oxygen was present. The reaction rate for copper (I) oxide is similar to that for an oxidized metallic copper catalyst, and the activation energy for an oxidized metallic copper catalyst is between the values for an unoxidized metallic copper catalyst and copper (I) oxide. The difference between the two catalysts is that the energy barrier for subsurface oxygen in metallic copper to diffuse to the surface and react is lower than the dissociation energy of copper (I) oxide into metallic copper and an oxygen atom. We do not see any change in the oxidation state of copper (I) oxide during the reaction and so believe that no dissociation occurs. The reaction on an oxidized metallic copper was explained by a model where adsorbed CO reacts with adsorbed oxygen and oxygen inhibits CO adsorption. This is what we believe happens on copper (I) oxide; the higher activation energy could be due to the extra energy needed to dissociate O_2 on the copper (I) surface. There is one study which reports that the heat of adsorption of CO on copper (I) oxide is greater than on metallic copper (27). The higher heat of adsorption of CO on copper (I) oxide, as compared to metallic copper, could be due to a lower surface coverage as heats of adsorption typically decrease with increasing coverage. The higher heat of adsorption does indicate that CO should be present on the surface during the reaction. The presence of oxygen on the copper (I) oxide surface can be inferred from its ability to further oxidize to copper (II) oxide, because in order to further oxidize, the copper (I) oxide surface must be able to dissociate O_2.

(*3*) *Reactions over copper (II) oxide.* CO oxidation over a copper (II) oxide catalyst has been studied by many researchers (12–17), but there is no consensus as to the mechanism. There is an agreement that the reaction rate is enhanced by exposing the catalyst to a reducing pretreatment. This work has shown that with decreasing copper oxidation state the CO oxidation rate is faster, in agreement with the enhancement found by reducing the catalyst surface. The possibility that different pretreatments may result in the catalyst surface having an oxidation state between 0 and 2 can explain why a consensus on the reaction mechanism has not been reached. It should also be mentioned that the catalyst surface might change depending on the gas phase composition during the reaction, as was demonstrated in Fig. 4, where metallic copper under a 66/33 CO/O_2 ratio at 275°C oxidized to copper (II) oxide. If a reaction was carried out where metallic copper was the starting catalyst and it was tested under stoichiometric reaction conditions, then the catalyst would change with time. If the reaction rate was measured at the start of the reaction or after some period, then different activation energies would be obtained from an Arrhenius plot. This fact complicates the interpretation of the current literature.

Combining our results for the oxidation of copper and the kinetic results obtained for CO oxidation under a 66/33 CO/O_2 ratio, we propose a redox cycle mechanism between CuO and Cu_2O where the rate limiting step is the reduction of copper (II) oxide by CO. We know that the reaction rate has a first order dependence in CO and that the reaction only proceeds if there is adsorbed CO on the catalyst surface (12). This indicates that the reaction is dependent on the surface coverage of CO. The adsorbed CO must react with either a gas phase oxygen or a surface oxygen. O_2 dissociation only occurs when electrons are donated from the surface to the O_2 molecule, leading to a metal cation and oxygen anion pair (28). Because copper (II) oxide is an insulator and cannot donate electrons, oxygen will not dissociate. Hence, for there to be CO_2 production, CO must reduce the catalyst surface. Under reaction conditions, where the ratio of CO to O_2 is less than or equal to 2, the surface will be rapidly oxidized to copper (II) oxide. The oxidation of the catalyst surface is faster than the reaction rate, which equals the rate of surface reduction. The deactivation in our kinetic results is due to CO_2 adsorption on the copper (II) oxide surface (14). CO_2 could be blocking CO adsorption sites on the surface or decomposing on a reduced surface site to adsorbed CO and oxygen. We believe the decomposition is unlikely because the high O_2 gas phase partial pressures would rapidly oxidize any reduced surface sites.

(*4*) *Comparison of the copper catalysts and platinum.* CO oxidation over platinum and the other noble metals has been a well-studied reaction and is therefore a good reference to compare with metallic copper, copper (I) oxide, and copper (II) oxide. For an excellent review of CO oxidation over the noble metals, the reader is referred to the work of Engel and Ertl (29). The mechanism

for CO oxidation over platinum is of the Langmuir–Hinshelwood type and has two regimes. The regimes are divided by the temperature of maximum CO desorption from the surface. At temperatures less than the desorption maximum, CO is adsorbed on the surface and the reaction rate law has a negative first order dependence on gas phase CO, and a positive first order dependence on gas phase oxygen. Adsorbed CO inhibits O_2 adsorption, which explains the pressure dependences. At temperatures greater than the desorption maximum, CO is not adsorbed on the surface allowing oxygen to saturate the surface. The reaction has a first order dependence on CO. In this study, platinum was tested under conditions where the temperature of the reactions was lower than the temperature for CO desorption. Hence, the surface is covered with adsorbed CO, which inhibits O_2 adsorption giving the previously mentioned partial pressure dependences (24).

The adsorption of CO and O_2 onto the copper catalyst surfaces is different from the platinum surface. For the reactions over the copper catalysts there is a positive dependence on the CO gas phase pressure. CO is weakly bound to the copper catalysts at these temperatures and pressures. Higher CO gas pressures will result in an increased surface coverage of adsorbed CO and a faster rate. We see no pressure dependence on O_2 for the reactions over the copper catalysts. There is an O_2 pressure dependence on the oxidation of the copper surface. The lack of a pressure dependence on O_2 for CO oxidation can be explained by the abundance of surface oxygen on the copper surface. Hence, CO oxidation over the copper catalyst is similar to a platinum catalyst run at temperatures greater than the CO desorption maximum temperatures.

Although the copper catalysts have similar pressure dependences, the activation energies differ for CO oxidation over all of the catalysts. If one starts with the assumption that the mechanism for CO oxidation over the three different copper catalysts is Langmuir–Hinshelwood like platinum, then the apparent activation energy, E_{App}, should equal the difference between the energy need for the Langmuir–Hinshelwood step, E_{LH} (reaction of adsorbed CO and adsorbed O), and the heat of adsorption of CO, E_{CO}:

$$E_{App} = E_{LH} - E_{CO}.$$

We measured a decrease in E_{App} with increasing copper oxidation. If E_{LH} is constant for all three copper catalysts, then E_{CO} would have to decrease with increasing oxidation. It was reported (27) that the heat of adsorption of CO on copper (I) oxide was greater than that on metallic copper. This means that the assumption that E_{LH} is constant is not valid. We might expect E_{LH} to differ on the different copper surfaces because of the changes in the bonding of oxygen to copper. This was demonstrated in the ability to reduce oxidized metallic copper but not copper (I) oxide during the reactions. Also, the three different copper catalysts were tested under different CO gas phase concentrations. This affects the amount of CO adsorption and therefore the CO heat of adsorption on the different copper surfaces. Last, a Langmuir–Hinshelwood reaction requires adsorbed oxygen on the surface, and in the case of copper (II) oxide, we believe that the oxygen in the reaction comes from the catalyst. This implies that the different activation energies are due to different reaction mechanisms.

The reaction rates for CO oxidation over the copper catalysts also changed with surface oxidation. The reaction rate decreases with increasing surface oxidation. The kinetics of copper (II) oxide have been most often compared in the literature to a platinum catalyst as a potential substitute. A review by Kummer (30) showed copper (II) oxide to be approximately 10 times less active, but at 100°C lower in temperature. Under similar conditions to Kummer's, we measured copper (II) oxide to be approximately 100 times less active. These results are not corrected for the different surface areas between the copper (II) oxide film and the platinum foil. This leads to the question of comparing surface areas or active sites between the three copper catalysts. Unfortunately, a measurement of the surface area or number of active sites on such a small amount of the oxidized copper catalysts is very difficult and could not be made. We believe that upon oxidizing the metallic copper catalyst to copper (I) and copper (II) oxide, there is a loss in active sites, giving rise to the possibility that turnover frequencies may be similar between the copper catalysts.

CONCLUSION

The three oxidation states of copper were formed and tested for the catalytic ability to oxidize CO to CO_2 using O_2. Metallic copper was generated by depositing the metal in UHV onto a graphite-coated stainless steel foil. XPS showed that copper (II) oxide was formed by oxidizing metallic copper in a 100 Torr of oxygen at 300°C for 20 min. and copper (I) oxide was formed by annealing copper (II) oxide at 400°C for 10 min. in UHV. AES showed that upon increasing oxidation, copper wets the graphite substrate. Under reaction conditions of 66/33 CO/O_2 partial pressure ratio at 275°C, metallic copper completely oxidizes to copper (II) oxide in approximately 1 hr. In order to prevent the oxidation state of the copper catalysts from changing during a catalytic test, the CO/O_2 ratio was fixed at 97/3, 90/10, and 66/33 Torr for metallic copper, copper (I) oxide, and copper (II) oxide, respectively. Metallic copper was found to be the most active, and with increasing copper oxidation the activity decreased. The

activation energy showed a reverse trend and increased with increasing oxidation. Metallic copper compared favorably to a platinum sample having a faster rate for temperatures less than 350°C and a lower activation energy. Copper (I) and copper (II) oxide were less active than the platinum sample but had lower activation energies. The mechanism for CO oxidation over the three copper catalysts was affected by subsurface oxygen and oxide formation.

ACKNOWLEDGMENT

This work was supported by the Director, Office of Energy Research, Office of Basic Energy Sciences, Material Sciences Division of the U.S. Department of Energy under Contract DE-AC03-76SF00098.

REFERENCES

1. Bowker, M., Houghton, H., and Waugh, K. C., *J. Chem. Soc. Faraday Trans. 1.* **77,** 3023 (1981).
2. Chinchen, G. C., Denny, P. J., Parker, D. G., Spencer, M. S., Waugh, K. C., and Whan, D. A., *Appl. Catal.* **30,** 333 (1987).
3. Campbell, C. T., and Daube, K. A., *J. Catal.* **104,** 109 (1987).
4. Colbourn, E., Hadden, R. A., Vandervell, H. D., Waugh, K. C., and Webb, G., *J. Catal.* **130,** 514 (1991).
5. Valyon, J., and Hall, W. K., *J. Phys. Chem.* **97,** 1204 (1993).
6. Ertl, G., Hierl, R., Knozinger, H., Thiele, N., and Urbach, H. P., *Appl. Surf. Sci.* **5,** 49 (1980).
7. Habraken, F. H. P. M., Kieffer, E. Ph., and Bootsma, G. A., *Surf. Sci.* **83,** 45 (1979).
8. Habraken, F. H. P. M., and Bootsma, G. A., *Surf. Sci.* **87,** 333 (1979).
9. Domagala, M. E., and Campbell, C. T., *Catal. Lett.* **9,** 65 (1991).
10. Van Pruissen, O. P., Dings, M. M. M., and Gizeman, O. L. J., *Surf. Sci.* **179** 377 (1987).
11. Dekker, N. J. J., Hoorn, J. A. A., Stegenga, S., Kapteijn, F., and Moulijn, J. A., *AIChE J.* **38,** 385 (1992).
12. Choi, K. I., and Vannice, M. A., *J. Catal.* **131,** 22 (1991).
13. Blumenthal, J. L., and Nobe, K., *Ind. Eng. Chem. Process Des. Dev.* **5,** 177 (1966).
14. Thomas, N. T., Caretto, L. S., and Nobe, K., *Ind. Eng. Chem. Process Des. Dev.* **8,** 282 (1969).
15. Prokopwicz, R. A., Silveston, P. L., Hudgins, R. R., and Irish, D. E., *React. Kinet. Catal. Lett.* **7,** 63 (1988).
16. Miro, E. E., Lombardo, E. A., and Petunchi, J. O., *J. Catal.* **104,** 176 (1987).
17. Pierron, E. D., Rashkin, J. A., and Roth, J. F., *J. Catal.* **9,** 38 (1967).
18. Marchon, B., Carrazza, J., Heinemann, H., and Somorjai, G. A., *Carbon* **26,** 507 (1988).
19. Hierl, R., Knozinger, H., and Urbach, H. P., *J. Catal.* **69,** 475 (1981).
20. Panzer, G., Egert, B., and Schmidt, H. P., *Surf. Sci.* **151,** 400 (1985).
21. Muilenberg, G. E., Ed., "Handbook of X-ray Photoelectron Spectroscopy," p. 82. Perkin–Elmer Corp., Eden Prairie, Minnesota, 1979.
22. Barr, T. L., *J. Phys. Chem.* **82,** 1801 (1978).
23. Brundle, C. R., *Faraday Discuss. Chem. Soc.* **60,** 159 (1975).
24. Berlowitz, P. J., Peden, C. H. F., and Goodman, D. W., *J. Phys. Chem.* **92,** 5213 (1988).
25. Labinger, J. A., and Ott, K. C., *Catal. Lett.* **4,** 245 (1990).
26. Bloch, J., Bottomley, D. J., Janz, S., and van Driel, H. M., *Surf. Sci.* **257,** 328 (1991).
27. Cox, D. F., and Schulz, K. H., *Surf. Sci.* **249,** 138 (1991).
28. Oudar, J., "Physics and Chemistry of Surfaces," p. 103. Blackie, Glasgow, 1975.
29. Engel, T., and Ertl, G., *Adv. Catal.* **28,** 2 (1979).
30. Kummer, J. T., *Proc. Energy Combust. Sci.* **6,** 177 (1980).